

# Oxidative Damage Precedes Nitrate Damage in Adriamycin-Induced Cardiac Mitochondrial Injury

LUKSANA CHAISWING,<sup>1,2</sup> MARSHA P. COLE,<sup>3</sup> DARET K. ST. CLAIR,<sup>3</sup> WANIDA ITTARAT,<sup>2</sup> LUKE I. SZWEDA,<sup>4</sup>  
AND TERRY D. OBERLEY<sup>1</sup>

<sup>1</sup>*Department of Pathology and Laboratory Medicine, William S. Middleton Memorial Veterans Administration Hospital and University of Wisconsin Medical School, Madison WI 53705, USA*

<sup>2</sup>*Faculty of Medical Technology, Mahidol University, Bangkok, 10700, Thailand*

<sup>3</sup>*Department of Toxicology, University of Kentucky, Lexington, KY 40506-0305, USA, and*

<sup>4</sup>*Department of Physiology and Biophysics, School of Medicine, Case Western Reserve University, Cleveland, OH 44106-4970, USA*

## ABSTRACT

The purpose of the present study was to determine if elevated reactive oxygen (ROS)/nitrogen species (RNS) reported to be present in adriamycin (ADR)-induced cardiotoxicity actually resulted in cardiomyocyte oxidative/nitrate damage, and to quantitatively determine the time course and subcellular localization of these postulated damage products using an *in vivo* approach. B6C3 mice were treated with a single dose of 20 mg/kg ADR. Ultrastructural damage and levels of 4-hydroxy-2-nonenal (4HNE)-protein adducts and 3-nitrotyrosine (3NT) were analyzed. Quantitative ultrastructural damage using computerized image techniques showed cardiomyocyte injury as early as 3 hours, with mitochondria being the most extensively and progressively injured subcellular organelle. Analysis of 4HNE protein adducts by immunogold electron microscopy showed appearance of 4HNE protein adducts in mitochondria as early as 3 hours, with a peak at 6 hours and subsequent decline at 24 hours. 3NT levels were significantly increased in all subcellular compartments at 6 hours and subsequently declined at 24 hours. Our data showed ADR induced 4HNE-protein adducts in mitochondria at the same time point as when mitochondrial injury initially appeared. These results document for the first time *in vivo* that mitochondrial oxidative damage precedes nitrate damage. The progressive nature of mitochondrial injury suggests that mitochondria, not other subcellular organelles, are the major site of intracellular injury.

**Keywords.** Adriamycin; 4-hydroxy-2-nonenal protein adducts; nitrotyrosine; reactive oxygen species; reactive nitrogen species; cardiac injury.

## INTRODUCTION

The anthracycline antibiotic adriamycin (ADR), or doxorubicin, is one of the most effective antitumor agents used to treat human malignancies. Long-term treatment with ADR is limited by cardiotoxicity. Many studies have demonstrated biochemical and pathological changes in heart following ADR treatment. Studies have suggested that mitochondria are an important subcellular target of ADR-induced cardiotoxicity. Disruption of mitochondrial cristae, mitochondrial swelling, and the presence of myelin figures within mitochondria were ultrastructural pathologic changes observed following treatment with ADR for 5 days (Yen et al., 1996). In addition, these changes were correlated with a significant functional decrease in state 3 respiration and respiratory control ratio in mitochondrial respiratory complexes I and II (Yen et al., 1999). Although these specific changes in mitochondria

could contribute to cardiac injury following ADR treatment, the specific subcellular sites responsible for cardiomyocyte injury have remained very controversial. Thus, myofibrils, sarcoplasmic reticulum (SR), and nuclei have all been proposed as primary sites of injury.

ADR has been shown to affect cardiac myofibrils by reduction of mRNA levels of cytoskeletal genes such as alpha actin, troponin I, and myosin light chain (Ito et al., 1990). These biochemical changes were correlated with ultrastructural analysis, which showed changes in myofibril structure, including loss, disruption, and disassembly of myofibrils. Recently, Mihm et al. (2002) have shown that cardiac myofibrils are a primary site of protein nitration following ADR treatment.

In addition, SR has also been suggested as a target for ADR-induced cardiotoxicity since depletion of the releasable SR calcium pool can be demonstrated following ADR treatment (Burke et al., 2002). Evidence against the SR as a major target of ADR is that overexpression of Ca<sup>2+</sup>-ATPase in the SR (SERCA2) in transgenic mice did not result in amelioration of ADR-induced cardiotoxicity (Burke et al., 2003).

ADR has been demonstrated to exert a multiplicity of effects on myocardial nuclei. Quantification of ADR-DNA adducts formation by <sup>32</sup>P-radiolabeled DNA has been demonstrated to be an early marker of ADR-induced cardiotoxicity (Hahm et al., 2003). Histological and ultrastructural studies have shown alterations in nucleoli after treatment with

Address correspondence to: Dr. Terry D. Oberley, Department of Pathology and Laboratory Medicine, William S. Middleton Memorial Veterans Administration Hospital, Rm A-35, 2500 Overlook Terrace, Madison, Wisconsin 53705. E-mail: toberley@wisc.edu; or Dr. Daret St. Clair, Department of Toxicology, University of Kentucky, 363 Health Sciences Research Building 0305, Lexington, Kentucky 40506-0305. E-mail: dstc1.00@pop.uky.edu

Abbreviations: ADR, adriamycin; 4HNE, 4-hydroxy-2-nonenal; 3NT, 3-nitrotyrosine; ROS, reactive oxygen species; RNS, reactive nitrogen species; NO, nitric oxide; ONOO<sup>-</sup>, peroxyxynitrite; and SR, sarcoplasmic reticulum.

ADR, including nucleolar segregation, nucleolar fragmentation, and conversion of nucleoli to a ring shape (Merski et al., 1976, 1978).

Since it is not certain which subcellular organelle(s) is (are) the primary target(s) of ADR-induced cardiotoxicity, one purpose of the present experiments was to determine the earliest subcellular target of ADR-induced cardiac injury using a time-course study and quantitative ultrastructural analysis of pathological lesions in mice. We propose that identification of the organelle(s) with the earliest and most prolonged injury will provide clues concerning the mechanism(s) of ADR-induced cardiac injury. A second major purpose was to correlate injury with analysis of oxidative/nitrative damage products *in vivo*.

The biochemical mechanism(s) by which ADR induces cardiotoxicity has not been fully elucidated. Many mechanisms have been proposed to explain ADR-induced cardiotoxicity, including the affinity of ADR to lipids, calcium concentration and membrane depolarization, disorder of membranes, free radical production, injury due to its metabolite (doxorubicinol), and disturbances in iron metabolism (Cummings et al., 1991; Forrest et al., 2000; Kwok and Richardson, 2002). Free radical production has been proposed to play a major role in ADR-induced cardiotoxicity. It has been demonstrated that ADR is a free radical generating agent due to its quinone structure (Sato et al., 1977). Many endogenous enzymes such as cytochrome P450, NADH dehydrogenase, and nitric oxide synthase have been demonstrated to catalyze the conversion of the ADR quinone structure to semiquinone free radicals (Doroshov, 1983; Doroshov et al., 1985; Weinstein et al., 2000). Semiquinone free radicals are rapidly oxidized in the presence of oxygen to produce superoxide radicals ( $O_2^{\cdot-}$ ). Further, superoxide radicals can react with other reactive oxygen species (ROS)/reactive nitrogen species (RNS) to form even more highly reactive ROS/RNS. Several investigators have also demonstrated the capacity of ADR to induce RNS production. Weinstein et al. (2000) have shown recently that peroxynitrite is formed in cardiomyocytes in mice after treatment with ADR, and Aldieri et al. (2002) have demonstrated that ADR induced nitric oxide synthesis with the resultant accumulation of nitrite in cells.

While the prior studies show the presence of ROS/RNS in ADR treated tissues, interpretation of results is not straightforward. First, most of the studies were performed in tissue homogenates: in these type of studies, the cell types and subcellular sites of ROS/RNS production cannot be identified. Second, the presence of ROS/RNS does not prove they are causative in the mechanism(s) of damage. In fact, ROS/RNS can have physiological functions. Third, increased ROS/RNS may be neutralized by the complex intracellular antioxidant defense system, and so oxidative stress may be present but not result in oxidative damage. The only way to prove that increased ROS/RNS cause cellular damage is to directly measure oxidative damage products *in situ* when they are bound to macromolecules, since adduct formation to protein or DNA is well recognized to cause cell injury.

4-Hydroxyl-2-nonenal (4HNE) is a major oxidative product derived from the breakdown of polyunsaturated fatty acids and related esters (Zainal et al., 1999). Further, 4HNE has been shown to have physiologic roles in cell proliferation and differentiation (Page et al., 1999), and this compound

may cause cellular damage by modification of intracellular proteins (Toyokuni et al., 1994). Moreover, it has previously been shown that treatment of purified protein with 4HNE leads to enzyme inactivation and protein cross-linking (Tsai et al., 1998). Intracellular 4HNE reacts rapidly with cysteine, lysine, and histidine residues of proteins (Spitz et al., 1991; Doorn and Petersen, 2002). Therefore, increase in 4HNE protein adducts not only indicates free radical production but also the subsequent interaction of oxidized lipids with proteins.

It has been shown that protein nitration is due to increases in ROS/RNS levels. 3-Nitrotyrosine (3NT) has served as a marker of the production of reactive nitrogen-centered oxidants ( $ONOO^-$ ,  $\cdot NO_2$ , etc.). Nitration of active-site tyrosine residues has been proven to alter protein structure and function (Kong et al., 1996; Ara et al., 1998). Under pathological conditions, 3NT has been suggested to modify both translational and posttranslational protein processes (Hanafy et al., 2001; Metzen et al., 2003; Willard et al., 2003).

Therefore, the detection of these two biomarkers (4HNE-protein adducts and 3NT) following ADR treatment would provide strong evidence for the actual presence of oxidative/nitrative damage. Our experiments were designed to measure immunoreactive 4HNE protein adducts and 3NT protein levels using specific antibodies and immunogold labeling with image analysis techniques in mice following treatment with ADR at various time points. The use of immunogold labeling with image analysis techniques not only allows identification of intracellular sites where injury has occurred, but also permits a quantitative comparison of oxidative/nitrative damage products at the site(s) of injury in control versus treated animals. The high sensitivity, specificity, and reliability of our immunogold techniques have been previously confirmed (Zainal et al., 2000). The concept of site-specific formation of oxidative/nitrative damage products in the cell is highly relevant for the understanding of how ADR injures cardiac tissues.

Our studies were performed in an acute animal model of ADR toxicity. Although it takes months for cardiac fibrosis to occur in humans, we believe that it would be difficult to interpret biochemical changes in a chronic animal model of ADR-induced cardiac toxicity since changes related to injury, repair, fibrosis, and adaptation would be impossible to separate from the original changes that caused cell injury. As an example, the major problem in studying human neurodegenerative diseases is that the only tissue available for analysis, for ethical reasons, is autopsy tissue. In tissues obtained at this end stage, it is difficult, if not impossible, to analyze early changes causing these diseases. For these reasons, we believe the acute model of ADR-toxicity is more relevant.

The present study is novel and important because it proves that oxidative/nitrative damage occurs at early time points *in vivo* in the heart following ADR treatment and provides quantitative results from various subcellular compartments; it demonstrates that oxidative damage precedes nitrative damage, which is consistent with the hypothesis of Mikkelen and Wardman (2003) that ROS changes are amplified by RNS changes; it demonstrates that mitochondria are the organelle showing the most progressive and extensive injury; and because oxidative injury in mitochondria precedes extensive cardiomyocyte injury, it suggests the possibility that ROS may be the cause of cardiomyocyte injury. In summary,

our results demonstrate that significant oxidative/nitrative posttranslational modifications of proteins occurred at early time points in cardiomyocyte mitochondria following ADR treatment.

#### MATERIALS AND METHODS

**Animals and Treatments:** Mice were from Jackson laboratory (Bar Harbor, ME) and housed at the animal facility of the University of Kentucky. Males from inbred B6C3 mice, age 10–13 weeks and weight 22–28 grams, were used for this study. In experiment 1, for both ultrastructural pathology and immunogold analysis, mice were injected intraperitoneally with 1 dose of either ADR (Pharmacia and Upjohn, Kalamazoo, MI) at 20 mg/kg (a dose that causes heart injury during the first 5 days but demonstrates low mortality rate,  $n = 2$  mice for each time point) or the same volume of saline (2.9% sodium chloride solution,  $n = 1$  mouse for each time point) as a control. Mice were euthanized by injection with 20 mg/kg of pentobarbital (Abbott Laboratories, North Chicago, IL) intraperitoneally at 4 different time points (0, 3, 6, 24 hours). Heart tissues from the left ventricle were then cut into 1-mm cubes and processed for further studies. The time period from euthanasia to placement of tissues into fixative was approximately 15 minutes. Thus, the time point labeled “zero” was actually approximately 15 minutes after the initial ADR dose; this lag period was present for each time point studied in the text.

In experiment 2, mice were treated with ADR ( $n = 2$  mice) or saline ( $n = 1$  mouse) and analyzed at 5 days for ultrastructural pathological analysis. The experimental procedures were approved by the Institutional Animal Care and Use Committee of the University of Kentucky.

**Morphometric Quantification by Electron Microscopy:** Heart tissues from the left ventricle were fixed, embedded, and processed for routine electron microscopy as previously described (Yen et al., 1996). Three embedded blocks from each heart for each mouse were sectioned and transferred to copper grids. Only longitudinal sections of cardiac muscle were used for the study. Grids were observed in an electron microscope (Hitachi H-600) operated at 75 kV. Random sampling was achieved by scanning the grid at low magnification so that cell injury was not apparent, yet gross sample artifacts (folds in tissues, dust particles, etc.) could be avoided. Grids were systematically scanned from top to bottom and from left to right so that photographs of entire cardiomyocyte cells were taken at  $\times 10,000$  magnification every 10–15 grid fields. Thirty cardiomyocyte cells were photographed for each mouse group. All quantitative ultrastructural data (mitochondrial or cytoplasmic damage) were analyzed from the same samples.

Mitochondria with any or several of the following ultrastructural criteria were used for determination of area involved by mitochondrial damage: mitochondrial swelling, mitochondria with the presence of myelin figures, mitochondria with loss of cristae, degeneration of mitochondria with disorganized cristae, lysosomal degradation of mitochondria, vacuolization in mitochondria, and mitochondrial membrane disruption. In the Results and Discussion sections, mitochondrial “damage” refers to mitochondria with any or several of the noted ultrastructural criteria. The data for mitochondrial

damage were presented as the average of the area involved by mitochondrial damage divided by the total area of mitochondria analyzed from 30 cells in each group at each time point.

Cytoplasm with any or several of the following ultrastructural criteria were used for identification of area involved by cytoplasmic damage: myofibrillar disorganization intracytoplasmic vacuolization, intracellular edema, the presence of myelin figures, and disruption of cell membranes. In the Results and Discussion sections, cytoplasmic “damage” refers to cytoplasm with any or several of the noted ultrastructural criteria. Cytoplasmic damage data was presented as the average of the area involved by cytoplasmic damage divided by the total cytoplasmic area from 30 cells in each group at each time point. The damaged areas of each subcellular compartments were measured in  $\mu\text{m}^2$  using image analysis software *Scion Image Beta 4.02* (Scion Corporation, Frederick, Maryland) with a PC computer (Dell OptiPlex GX200) as described previously (Oberley, 2002).

**Ultrastructural Localization and Relative Quantification of 4HNE Modified Protein Adducts, 3NT, and Beta-Actin:** Heart tissues from the left ventricle were fixed, embedded, and processed for immunogold electron microscopy as described previously in detail (Oberley, 2002). Two embedded blocks from each heart for each mouse were sectioned and transferred to nickel grids. Only longitudinal sections of cardiac muscle were used for the study. Grids were rinsed with TBS, blocked with BSA-C, and then washed with TBS. The grids were incubated with primary antibodies [rabbit anti-4HNE modified proteins polyclonal antibody (obtained from Dr. Luke Szweda, Case Western University, Cleveland, OH) diluted 1:80, rabbit anti-3NT antibody (Upstate Biotechnology, Lake Placid, NY) diluted 1:400, and rabbit anti-beta actin antibody (Santa Cruz Biotechnology Inc., Santa Cruz, CA) diluted 1:80] at 4°C overnight in a humidified chamber. The grids were incubated with diluted (1:75) gold conjugated secondary antibody (15 nm gold conjugated goat anti-rabbit IgGH+L, BB International Cardiss, UK) for 90 minutes at room temperature. Grids were then rinsed in TBS, counterstained with uranyl acetate, observed, and photographed with an electron microscope (Hitachi H-600) operated at 75 kV.

For experimental grids stained with anti-3NT antibody, the rinsing step, blocking step, and incubation with the primary antibody were performed under a vacuum system to protect against the reactions of ROS/RNS with atmospheric oxygen and nitrogen. The reaction of nitric oxide with oxygen leads to nitrogen dioxide ( $\text{NO}_2$ ) production, which is known to nitrate tyrosine residues with  $K_m = 2.9 \times 10^7 \text{ [M}^{-1} \text{ s}^{-1}]$  in vivo (Halliwell, 1997; Kirsch et al., 2002). Even though the reaction rate is relatively slow in aqueous phase under physiological conditions, to protect against false positive results, the grid samples were kept under vacuum conditions before staining with the primary antibody. Samples not treated in this fashion showed increasing nonspecific labeling as a function of time after exposure to air (data not shown).

As a control, normal rabbit serum (1:1000, DAKO Inc., Carpinteria, CA) and antibody diluent (ScyTek, Logan, Utah) were used in place of the primary antibody; these controls resulted in trace background labeling (data not shown).

For relative quantification of the immunoreactive protein of interest (4HNE modified proteins, 3NT, and beta-actin) in

an experimental group versus a control group, all of the sections were stained simultaneously under the same conditions. Random sampling was achieved by scanning the grid at low magnification so that immunogold beads could not be seen, yet gross sample artifacts (folds in tissues, dust particles, etc.) could be avoided. Grids were scanned systematically from top to bottom and from left to right, and then photographs of entire cardiomyocyte cells were taken at  $\times 12,300$  magnification every 10–15 grid fields.

Photographs of 30 cardiomyocyte cells were taken from each mouse group. The areas of each compartment (mitochondria, cytoplasm, and nucleus) were outlined and measured by image analysis software as previously described (Zainal et al., 1999). Gold beads within specific subcellular compartments were then counted manually; over 1,000 gold beads were counted per group. The mean density of gold beads/ $\mu\text{m}^2$  area was expressed as mean value  $\pm$  SEM of 30 cardiomyocyte cells.

**Antibody Specificity:** Antibody for 4HNE-modified proteins has been previously described in detail (Uchida et al., 1993; Zainal et al., 1999, 2000). Rabbit polyclonal IgG anti-3NT was a commercial antibody that was raised against nitrated keyhole limpet hemocyanin. The specificity of this antibody was verified by pre-absorption with 5 mM 3NT for 3 hours at room temperature; cardiomyocytes showed no significant positive staining after pretreatment of antibody with antigen (data not shown). Anti-beta actin (internal control) antibody used was a commercial rabbit polyclonal antibody raised against a recombinant protein corresponding to amino

acids 180–375 mapping at the carboxyl terminus of beta-actin of human origin. Western blot analysis showed this antibody reacted with authentic beta-actin (unpublished results).

**Statistical Analysis:** Quantitative results were expressed as means  $\pm$  SEM. Statistical evaluations were performed with the SPSS10 for Windows program (SPSS Inc., Chicago, IL). Multiple comparisons of the 0 hour versus other time points were performed by a 1-way ANOVA followed by the post hoc test (LSD). Mean differences were considered significant at  $p \leq 0.05$  as indicated in the Results section and figures.

## RESULTS

### *Mitochondria are the Subcellular Organelle Most Extensively and Progressively Injured in Adriamycin-Induced Cardiac Toxicity*

Ultrastructural pathological examination of heart following saline treatment showed rare loss of mitochondrial cristae and swollen mitochondria. In contrast, ADR-treated mice showed dramatic subcellular changes, including mitochondrial vacuolization, the presence of myelin figures, intracytoplasmic vacuolization, and cellular and mitochondrial membrane disruption (Figure 1).

For quantitation of the degree of cardiac injury, we measured the areas of mitochondrial (Figure 2) and cytoplasmic damage in cardiomyocytes. Quantitative data are demonstrated in Figure 3. After exposure to ADR, mitochondrial damage was present as early as 3 hours and significantly increased at 6 and 24 hours ( $p$ -value  $\leq 0.05$  when compared

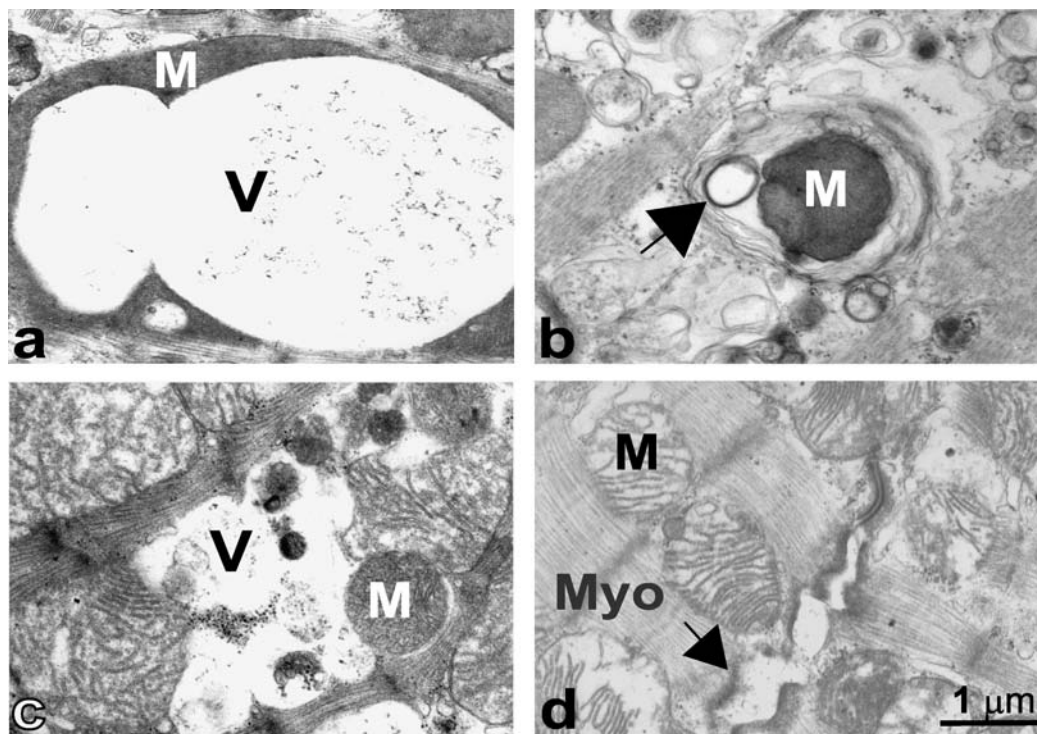


FIGURE 1.—Representative high magnification electron micrographs demonstrating ultrastructural lesions identified in mice treated with 20 mg/kg ADR. After injection with ADR, ultrastructural examination of mouse hearts at 24 hours showed significant pathologic changes including: vacuole within mitochondria (a), mitochondria with myelin figure (b, arrow), intracellular vacuolization (c), and membrane disruption resulting in separation of plasma cell membranes (d, arrow). M; mitochondria. V; vacuolization. Myo; myofibril.

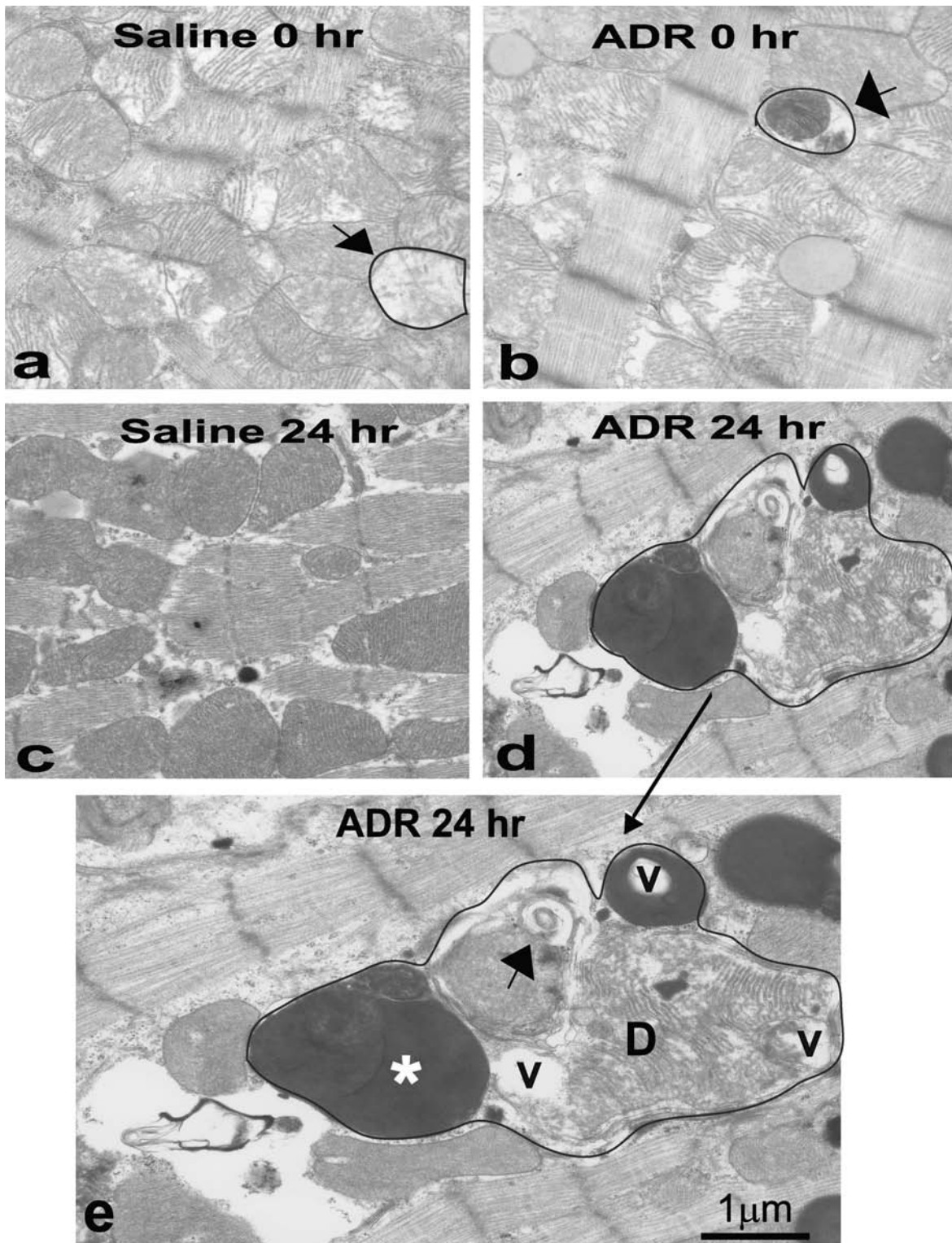


FIGURE 2.—Morphometric quantification of mitochondrial damage area ( $\times 10,000$ ). (a) Mice treated with saline at 0 hour demonstrated mitochondria with focal loss of cristae (arrow). (b) Mice treated with ADR at 0 hour demonstrated a few ultrastructural changes including mitochondria with disorganized cristae and vacuolization (arrow). (c) Mice treated with saline at 24 hours. (d) Mice treated with ADR at 24 hours demonstrated the most mitochondrial damage. (e) Higher magnification ( $\times 12,300$ ) of mitochondrial damage of mice treated with ADR at 24 hours, which included vacuolization in mitochondria (V), mitochondria with the presence of myelin figures (arrow), degeneration of mitochondria with disorganized cristae (D) and lysosomal degradation of mitochondria (\*). For each photograph, areas involved by mitochondrial damage were outlined. *Note:* mitochondria with focal loss of cristae (a) may represent fixation artifact or actual injured mitochondria.

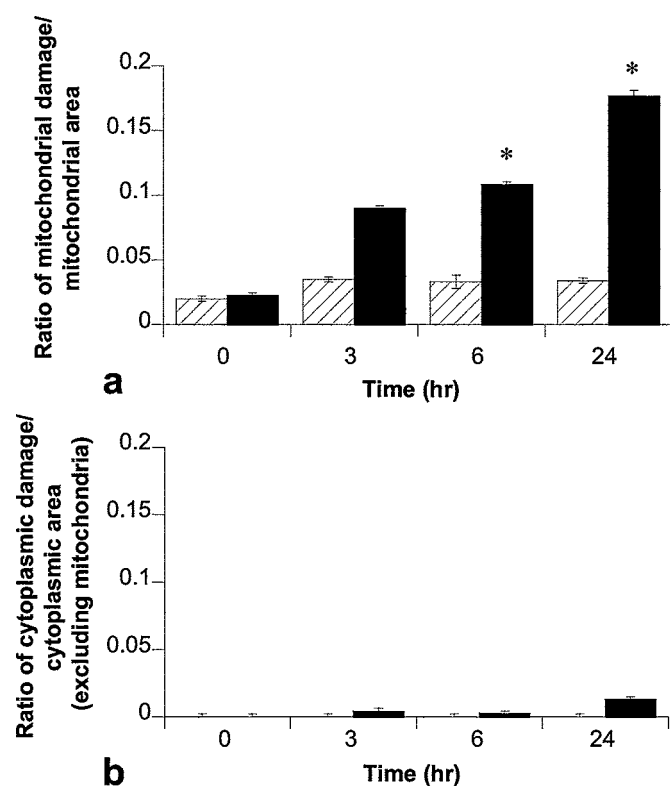


FIGURE 3.—Quantitative analysis of damaged areas in mice treated with ADR or saline at early time points. (a) Mitochondrial damage, (b) Cytoplasmic damage. Mitochondrial damage first appeared at 3 hours, significantly increased at 6 hours after treatment with ADR, and was further increased at 24 hours. Mitochondrial damage was greater than cytoplasmic damage. Cytoplasmic damage did not increase statistically when examined at the time points indicated. Mitochondrial damage of ADR treated mice was greater than saline treated mice. ADR, black bars, saline, striped bars. \* $p \leq 0.05$  when compared with 0 hour.

with 0 hour). Mitochondrial damage (areas involved by mitochondrial damage/total mitochondrial area) at 24 hours was increased about 8-fold when compared with mice treated with ADR at 0 hours. As shown in Figure 3, mitochondrial damage areas were greater than areas involved by cytoplasmic damage when compared at 24 hours (about 2-fold differences). There was no major difference in cytoplasmic damage of mice treated with ADR versus saline at any time points examined. In addition, we observed very little cytoplasmic damage in cardiac tissues treated with ADR at 24 hours. These data indicated that mitochondria were one major target of ADR-induced cardiac injury during the first 24 hours.

We also treated a different set of mice in a second experiment with ADR at 20 mg/kg or saline and analyzed cardiac tissues at 5 days to investigate whether a longer time period following ADR treatment resulted in greater cardiac injury. As shown in Figure 4, the data from mice treated with ADR at 5 days showed more injury in both categories (mitochondrial damage increased about 7-fold and cytoplasmic damage increased about 6-fold) than mice treated with ADR at 24 hours. These data demonstrated that damage initiated by a single dose of ADR resulted in progression of cardiac injury for at least 5 days. Comparing mitochondrial and cytoplasmic damage from 24 hours and 5 days after ADR treatment, mitochondrial damage was greater than cytoplasmic damage

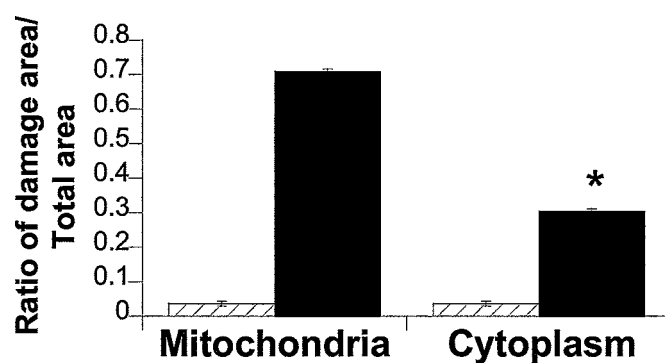


FIGURE 4.—Morphometric quantification of damaged areas in mice treated with 20 mg/kg ADR or saline treatment at 5 days. The ultrastructural lesions in cardiomyocytes were greatly increased in mice treated with ADR at 5 days in comparison with cardiomyocytes from saline-treated mice. Mitochondrial damage was significantly higher than cytoplasmic damage. All area data were measured in  $\mu\text{m}^2$ . ADR, black bars, saline, striped bar. \* $p \leq 0.05$  when cytoplasmic damage was compared with mitochondrial damage. Note that the Y-axis is greatly expanded (4 times) in Figure 4 relative to Figure 3 because of the large increase in damage.

at both time points with a consistent ratio between subcellular compartments (about 2-fold). These data suggested that the extensive damage observed in the cytoplasm was probably secondary to progressive mitochondrial damage.

#### *Quantitative Immunogold Ultrastructural Analysis Identifies Oxidative Damage of Proteins in Mitochondria as an Early Event in Adriamycin-Induced Cardiotoxicity*

To determine the effect of ADR on lipid peroxidation-modified proteins, the same set of mice used in the ultrastructural analyses described previously were utilized and immunogold analysis for 4HNE protein adducts was performed as described in Materials and Methods. Gold beads representing 4HNE protein adducts are demonstrated in Figures 5a and 5b and are seen in significant numbers over mitochondria. Significant label was also observed over myofilaments.

As shown in Figure 6a, there were low levels of immunoreactive 4HNE protein adducts in mice treated with saline at 6 hours, which could be related to 4HNE physiological functions. The results in Figures 6b and 6c demonstrated that immunoreactive 4HNE protein adducts were identified in mitochondria at time points before nuclei and cytoplasm, with the label in mitochondria being detected as early as 3 hours after treatment with ADR. In all 3 subcellular compartments, the maximal level of immunoreactive 4HNE protein adducts occurred at 6 hours (2.5–3-fold increase when compared with saline treatment in all 3 compartments), and then subsequently declined at 24 hours. These data indicated that 4HNE protein adducts in mitochondria were produced at an early time point following ADR treatment.

#### *Quantitative Immunogold Ultrastructural Analysis Identifies Nitrate Damage of Proteins in Mitochondria Following Adriamycin Treatment*

To determine the effect of ADR on protein nitration, the same set of mice used in the ultrastructural analysis and 4HNE studies described before were utilized and immunogold analysis for immunoreactive 3NT protein was performed as

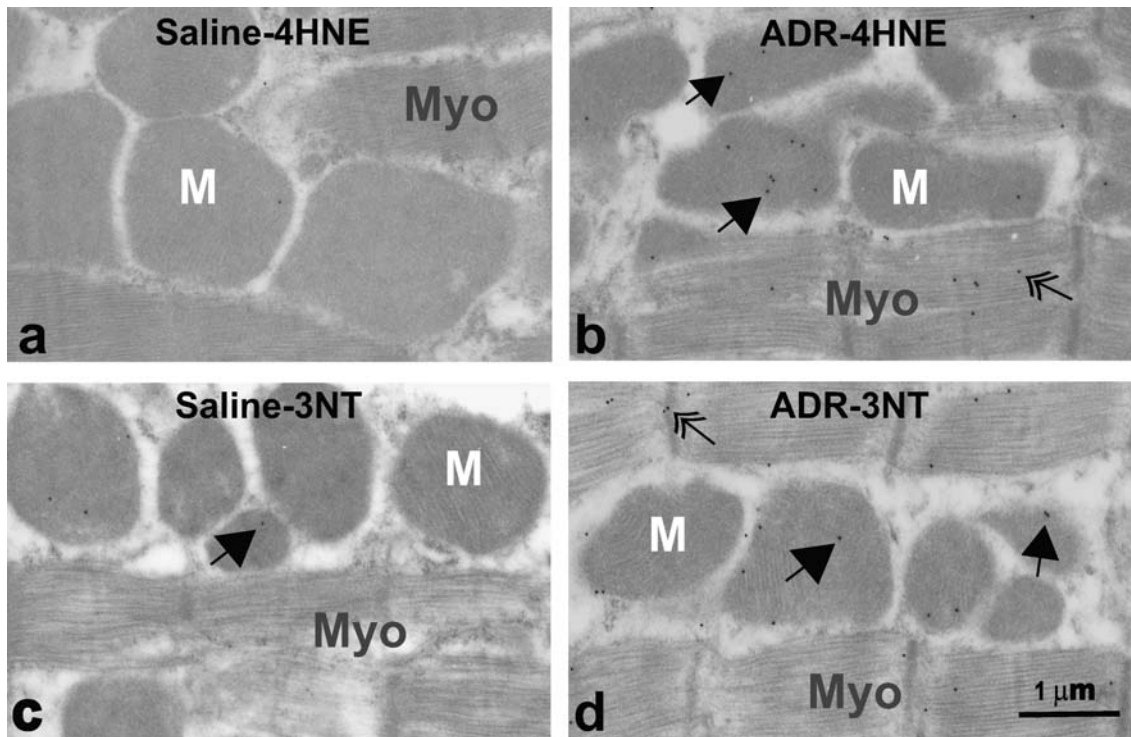


FIGURE 5.—Representative immunogold EM photographs using antibody against 4HNE-modified protein or 3NT in cardiomyocyte cells ( $\times 12,300$ ). Mice treated with saline demonstrated low labeling of 4HNE protein adducts (a) or 3NT (c) in all subcellular compartments. Mice treated with 20 mg/kg ADR showed significant labeling of 4HNE protein adducts (b) or 3NT (d) in mitochondria (M) and myofibrils (Myo). Arrows and double arrows point to gold beads, which indicated positive 4HNE protein adducts or 3NT labeling in mitochondria and myofibrils, respectively.

described in Materials and Methods. Gold beads demonstrating immunoreactive 3NT proteins are shown in Figures 5c and 5d.

As shown in Figure 7a, mice treated with saline showed that protein nitration in cardiomyocytes was localized more extensively to mitochondria than other subcellular compartments. Mice treated with saline did not show any significant differences in immunoreactive 3NT protein levels at 3, 6, and 24 hours in comparison to 0 hr treatment in all 3 compartments. In contrast, immunoreactive 3NT protein levels in ADR treated mice were increased significantly in all subcellular compartments at 6 hours following ADR treatment, with subsequent decline at 24 hours (Figures 7b and 7c). In contrast to 4HNE, analysis of the labeling density ratio of ADR/Saline for 3NT showed increased but equal ratios at 6 hours in all subcellular compartments (compare Figures 6 and 7). These data indicated that 3NT formation occurred in all subcellular compartments and at a later time point than 4HNE protein adducts.

#### *The Effect of ADR on the Housekeeping Protein Beta-Actin*

We have measured beta-actin immunoreactive protein levels by using specific antibody with immunogold labeling and image analysis techniques to confirm the fact that the alterations in our modified proteins of interest (4HNE and 3NT) were real and not due to changes in overall protein expression induced by ADR. Beta-actin labeling was found primarily over myofibrils. There were no significant differences in

beta-actin protein levels when comparing mice treated with ADR or saline at any time points (data not shown).

#### DISCUSSION

Our studies are the first to document and quantify levels of oxidative/nitrative damage products in situ in specific subcellular locations in cardiac tissues following ADR treatment. We established that ADR-induced 4HNE protein adduct formation in mitochondria occurred at an early time preceding protein nitration and extensive cell injury. Since 4HNE protein adducts are a marker of ROS formation and 3NT is a marker of combined RNS and ROS production, we hypothesized that an imbalance of ROS production in mitochondria at 3 hours stimulated  $\cdot\text{NO}$  production in all subcellular compartments at 6 hours with a coincident peak of mitochondrial injury at 3–6 hours. Our results are consistent with the hypothesis of Mikkelsen and Wardman (2003) that ROS changes are amplified by RNS changes. Time-course data in a second experiment indicated that injury identified 5 days after treatment with ADR was more prominent than injury observed 1 day after treatment.

Our ultrastructural time course data demonstrated for the first time that mitochondria were an early and the most extensively and progressively injured organelle in ADR-induced cardiotoxicity. These results are consistent with a previous qualitative analysis conducted in our laboratory (Yen et al., 1996). Moreover, our studies did not find any significant difference in the degree of injury between subsarcolemmal

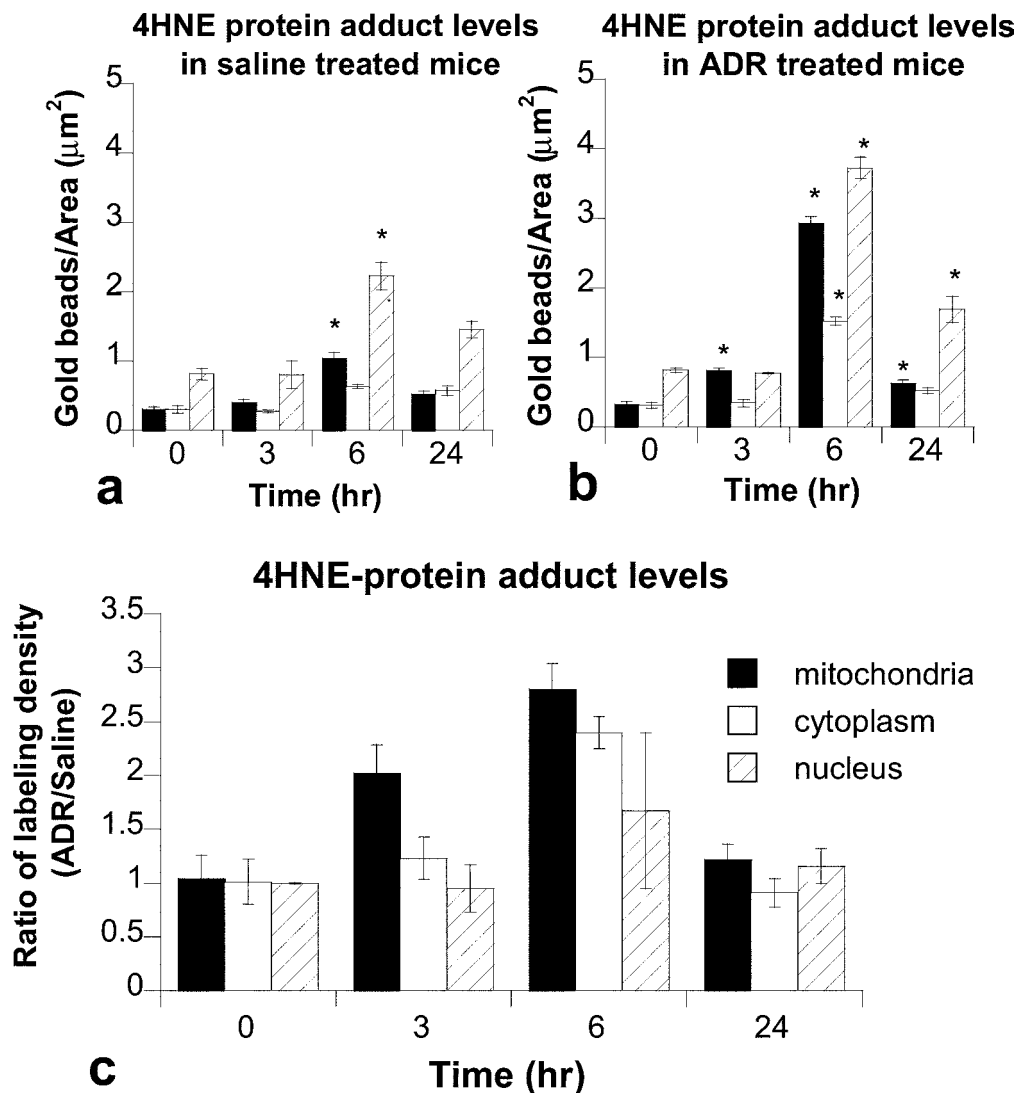


FIGURE 6.—Quantitative analysis of density of 4HNE gold labeling. (a) Mice treated with saline; (b) Mice treated with ADR at 20 mg/kg; and (c) Ratio of labeling density (ADR/Saline). Immunoreactive 4HNE protein adducts were present in all subcellular compartments. Levels were higher after ADR treatment in mitochondria as early as 3 hours with a peak at 6 hours, with subsequent decline at 24 hours. \* $p \leq 0.05$  when compared with 0 hours.

mitochondria (beneath the sarcolemma membrane) and interfibrillar mitochondria (between the myofibrils) (data not shown), providing an internal control that the mitochondrial injury identified was not due to sampling techniques. The cardiac mitochondrial ultrastructural damage identified in our experiments in ADR-treated mice may correlate with reported biochemical changes in injured mitochondria, such as permeability changes in the mitochondrial membrane, electrolyte transport dysfunction, alterations in respiratory chain enzyme activities, decrease in ATP content and/or reduction in oxygen consumption (Aversano and Boor, 1983).

While the present study established that mitochondrial injury is an important event in ADR toxicity, other subcellular compartments have been shown to be damaged in ADR-induced cardiotoxicity. For example, Ito et al. (1990) demonstrated that myocardial injury resulting from treatment with ADR was characterized by significant myofibril loss and

sarcotubular swelling. However, Ito et al. (1990) studied myocardial injury after treatment with ADR for 8 days, which was only one time point and longer than our experimental design. Our experiments have also shown an increase in cytoplasmic injury, including loss of myofibrils, and myofibrillar disorganization following treatment with ADR, but the myofibrillar injury was less extensive than mitochondrial injury and occurred at a later time point (specifically 5 days after ADR treatment). Overall, our results may be explained by the possibility that increasing mitochondrial damage at later times following ADR treatment may result in more extensive myofibrillar damage. Therefore, myofibrillar injury may be a secondary event after primary mitochondrial dysfunction. In fact, mitochondrial dysfunction can lead to imbalance of  $\text{Ca}^{2+}$  uptake and loss of ATP production, factors that are known to be important in normal myofibrillar function (Gosalvez et al., 1974; Revis and Marusic, 1979).

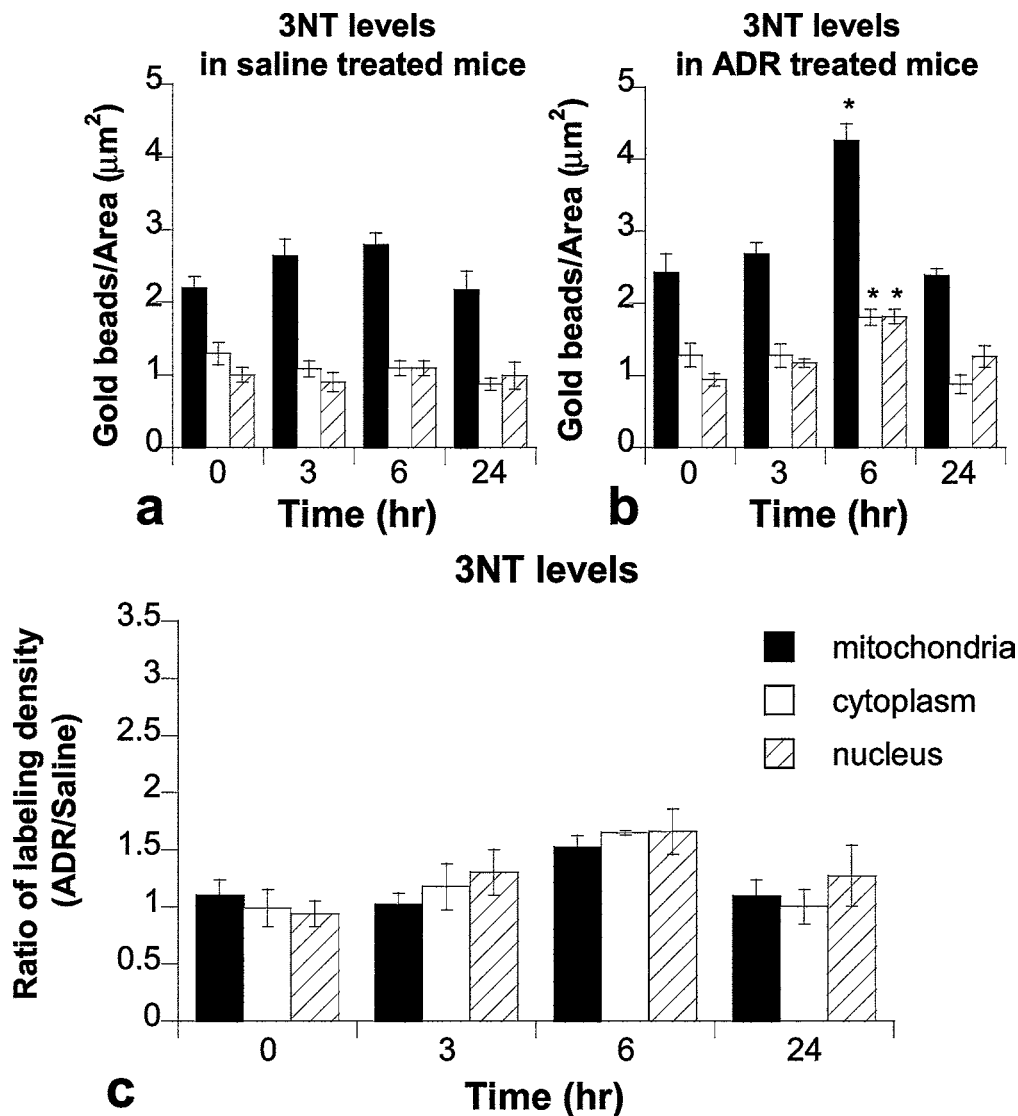


FIGURE 7.—Quantitative analysis of density of 3NT gold labeling. (a) Mice treated with saline (b) Mice treated with ADR at 20 mg/kg (c) Ratio of labeling density (ADR/Saline). Protein nitration (3NT) was present in all subcellular compartments. 3NT levels were increased after ADR treatment in all compartments at 6 hours, with subsequent decline at 24 hours. \* $p \leq 0.05$  when compared with 0 hours.

Many studies have established that nuclear changes occurred in ADR-induced cardiotoxicity. Histological and ultrastructural studies have shown alterations in the nucleolus after treatment with ADR, including nucleolar segregation, nucleolar fragmentation, and conversion of nucleoli to a ring shape (Lambertenghi-Delilieri et al., 1976; Merski, 1976). We did not observe apoptotic nuclei or major nucleolar morphologic changes in our experiments. However, we observed small changes in nuclear and nucleolar areas following ADR treatment at 6 and 24 hours respectively (data not shown). These changes were not extensive enough to account for changes in labeling density and were not progressive as observed with mitochondrial damage.

Many studies have suggested that ROS are a primary cause of ADR-induced cardiotoxicity. Although it is known that ROS and RNS are increased in heart following ADR treatment, and it has been demonstrated that ROS/RNS can inactivate cardiac enzymes *in vitro*, the exact significance of

these studies is questionable since there are extensive defense systems against ROS that could protect against increased ROS/RNS *in vivo*. The present study proved that these defense systems were not sufficient to protect against ROS/RNS since oxidative/nitrative damage products were detected *in situ* using a technique that was suitable to address this problem, i.e., quantitative immunogold electron microscopy. We demonstrated in previous studies [in Rhesus monkeys with a large number of animals (Zainal et al., 2000)] a tight correlation between our immunogold labeling procedure and biochemical analysis.

Our data indicated that immunoreactive 4HNE protein adducts were present in both physiological (low levels of immunoreactive 4HNE protein adducts in mice treated with saline) and pathological conditions (high levels of immunoreactive 4HNE protein adducts after treatment with ADR). Treatment of mice with ADR resulted in immunoreactive 4HNE protein adducts formation in cardiac mitochondria at

very early times after treatment (3 hours). Western blot analysis confirmed an increase in 4HNE protein adducts in cardiac tissues of ADR vs. saline treated mice, thus confirming the immunogold analysis presented in this study (data not shown); the information gained from Western analysis was limited since whole cell homogenates were used and thus the subcellular localization of 4HNE-protein adducts could not be determined. The early elevation of lipid peroxidation-modified protein formation in mitochondria correlated with an increase in mitochondrial injury at similar time points. Several proteins, lipids, and metabolic enzymes in mitochondria can be inactivated through modification by ROS (Reinheckel et al., 1998). Similarly, free 4HNE and many aldehydes can also act as toxic molecules, since they are reactive and diffusible. 4HNE protein adducts in cell membranes have been shown to cause changes in cell membrane fluidity and integrity; these changes have been shown to modify membrane protein functions, including ATP-ase activity,  $\text{Na}^+$ - $\text{K}^+$  ion pump activity, and functioning of the membrane transport system (Chiarpotto et al., 1999; Fleurbaey-Morel et al., 1999; Paola et al., 2000; Singhal et al., 2003). Moreover, 4HNE protein adducts have been demonstrated to alter mitochondrial energy metabolism in heart (Poli et al., 1985; Nguyen and Picklo, 2003). Recently, Benderdour et al. (2003) have shown that cardiac mitochondrial  $\text{NADP}^+$  isocitrate dehydrogenase is a target for modification by 4HNE following oxidative stress. Biochemical alterations of membrane proteins may precede pathological changes, such as disruption of cell membranes, cell swelling, and intracellular vacuolization (Cotran et al., 1999). Moreover, free 4HNE may function as a signal transduction molecule by activation of inflammatory cytokines and chemokines, with resultant injury to cardiac tissues (Parola et al., 1993).

In the present study, immunoreactive 4HNE protein adducts subsequently declined at 24 hours after ADR treatment. Superoxide radical, hydroxyl radical, lipid, protein, and iron are necessary for 4HNE protein adduct formation. Studies have also shown that free 4HNE is a chemoattractant and rapidly destroyed by white blood cells (Curzio, 1988); however, in our studies, we did not observe any white blood cell infiltration in cardiac tissues. We suggest that at 24 hours 4HNE protein adducts may have been removed by the proteasome (Grune et al., 1995) and/or lysosome systems in the cell. However, ultrastructural cellular injury at 24 hours was not reduced; this result is consistent either with the hypothesis that 4HNE protein adducts are not causal in ADR-injury or that the oxidative damage needs to be present for only a short time to cause prolonged injury. Previous *in vitro* studies suggest that the latter possibility is correct; in model systems, it was demonstrated that 90% of adduct aldehydes disappeared rapidly within 10 minutes, whereas the injury effects appeared after 1–4 hours and could be prolonged for a few days even though no trace of aldehydes could be detected (Barrera et al., 1994, 1996; Dianzani, 1998).

We also studied nitrative damage in cardiomyocytes following ADR treatment. 3NT has served as a marker of the production of reactive nitrogen-centered oxidants ( $\text{ONOO}^-$ ,  $\text{NO}_2$ , etc.). In the present study, we demonstrated the presence of immunoreactive 3NT protein in all 3 subcellular compartments in mice treated with saline, which indicated physiological functions of RNS. Interestingly, under these

conditions, mitochondria had higher 3NT levels than the cytoplasm or nucleus.  $\text{NO}$  has been demonstrated to be a modulator of cardiac oxygen consumption, mediated through reduction of cytochrome oxidase complex I and II activities (Granger and Lehninger, 1983; Burcham, 1998; Brown, 2001). The significant levels of 3NT found in mitochondria of mice treated with saline may be the result of physiological events in which peroxynitrite is present at low levels.

We have shown that 3NT was present at increased levels in cardiomyocytes following ADR treatment. The 3-Nitrotyrosine was shown to increase in cardiomyocytes at 6 hours after ADR treatment and then declined at 24 hours. The 3NT formation was observed in all subcellular compartments. We hypothesize that the increase in immunoreactive 3NT protein observed was due to the reaction of  $\text{NO}$  with superoxide radical to form peroxynitrite and other RNS. It is not certain that 3NT results only from the formation of peroxynitrite, but peroxynitrite is the most likely source *in vivo* (Beckman et al., 1994). Increased production of either  $\text{NO}$  or superoxide radical may be sufficient to cause the formation of these species.  $\text{NO}$  may increase levels of oxidative stress by generation of peroxynitrite, a highly cytotoxic oxidant, but paradoxically may decrease the levels of oxidative stress by neutralizing the toxic superoxide radical and preventing iron-catalyzed hydroxyl radical formation. In addition,  $\text{NO}$  has been shown to protect cells against hydrogen peroxide-mediated injury by regulation of mitochondrial respiration, which may lead to the maintenance of mitochondrial membrane potential following injury and hence prevent apoptosis (Paxinou et al., 2001). Likewise, there are several mitochondrial proteins that can rapidly react with  $\text{NO}$ , examples being metalloproteins, cytochromes, and thiol proteins (Brown, 2001; Costa et al., 2003; Thomas et al., 2003). The nitration of these proteins can modulate their functions. However, which protein(s) is the actual target for tyrosine nitration needs to be the subject of further study.

Using similar immunogold labeling techniques, our 3NT data are in contrast with the studies of Mihm et al. (2002), which demonstrated that at 5 days after treatment of mice with 20 mg/kg ADR, the density of immunoreactive 3NT protein levels in cardiac myofibrils was higher than that found in mitochondria. Our studies have also shown immunoreactive 3NT protein levels in myofibrils were significantly increased at 6 hours after treatment with ADR but levels were less than levels in mitochondria. The study of Mihm et al. (2002) did not protect tissue from air, which may explain the discordant results.

Our data indicated that ADR induced lipid peroxidation in mitochondria at early times, with subsequent nitrative damage product formation in all subcellular compartments and extensive cell injury at later times. Therefore, mitochondria are a primary site of oxidative/nitrative damage products and the organelle most extensively and progressively involved in ADR-induced cardiotoxicity. The injury to the other organelles appears to be a secondary event after the injury to mitochondria. An understanding of how ROS/RNS affect ADR-induced cardiotoxicity is a requirement for evaluating the role of antioxidants in protection against cardiomyocyte injury. Moreover, cardiomyocyte mitochondria are postulated to represent the major source of ROS/RNS production during ADR-induced cardiotoxicity. These free radicals cause

extensive oxidation and nitration of proteins. However, which protein target(s) are most responsible for cellular injury remains to be established.

#### ACKNOWLEDGMENTS

This work was supported in part by grants to Drs. Daret St. Clair and Terry Oberley from The National Institutes of Health (CA 49797 and CA 59835), to Luksana Chaiswing from Thailand Research Fund under the Royal Golden Jubilee program, and to Marsha Cole from a training grant in oxidative stress and nutrition (T32DK07778). The work was supported in part by resources and the use of facilities at the William S. Middleton Memorial Veterans Hospital, Madison Wisconsin. We gratefully thank Dr. Larry W. Oberley for critical review of this manuscript.

#### REFERENCES

- Aldieri, E., Bergandi, L., Riganti, C., Costamagna, C., Bosia, A., and Ghigo, D. (2002). Doxorubicin induces an increase of nitric oxide synthesis in rat cardiac cells that is inhibited by iron supplementation. *Toxicol Appl Pharmacol* **185**, 85–90.
- Ara, J., Przedborski, S., Naini, A. B., Jackson-Lewis, V., Trifiletti, R. R., Horwitz, J., and Ischiropoulos, H. (1998). Inactivation of tyrosine hydroxylase by nitration following exposure to peroxynitrite and 1-methyl-4-phenyl-1,2,3,6-tetrahydropyridine (MPTP). *Proc Natl Acad Sci USA* **95**, 7659–63.
- Aversano, R. C., and Boor, P. J. (1983). Histochemical alterations of acute and chronic doxorubicin cardiotoxicity. *J Mol Cell Cardiol* **15**, 543–53.
- Bachman, E., Weber, E., and Zbinden, G. (1975). Effects of seven anthracycline antibiotics on electrocardiogram and mitochondrial function of rat hearts. *Agents Actions* **5**, 383–93.
- Bachur, N. R., Gordon, S. L., and Gee, M. V. (1977). Anthracycline antibiotic augmentation of microsomal electron transport and free radical formation. *Mol Pharmacol* **13**, 901–10.
- Barrera, G., Muraca, R., Pizzimenti, S., Serra, A., Rosso, C., Saglio, G., Farace, M. G., Fazio, V. M., and Dianzani, M. U. (1994). Inhibition of c-myc expression induced by 4-hydroxynonenal, a product of lipid peroxidation, in the HL-60 human leukemic cell line. *Biochem Biophys Res Commun* **203**, 553–61.
- Barrera, G., Pizzimenti, S., Serra, A., Ferretti, C., Fazio, V. M., Saglio, G., and Dianzani, M. U. (1996). 4-Hydroxynonenal specifically inhibits c-myc but does not affect c-fos expressions in HL-60 cells. *Biochem Biophys Res Commun* **227**, 589–93.
- Beckmann, J. S., Ye, Y. Z., Anderson, P. G., Chen, J., Accavitti, M. A., Tarpey, M. M., and White, C. R. (1994). Extensive nitration of protein tyrosines in human atherosclerosis detected by immunohistochemistry. *Biol Chem Hoppe Seyler* **375**, 81–8.
- Benderdour, M., Charron, G., DeBlois, D., Comte, B., and Des Rosiers, C. (2003). Cardiac mitochondrial NADP<sup>+</sup>-isocitrate dehydrogenase is inactivated through 4-hydroxynonenal adduct formation: an event that precedes hypertrophy development. *J Biol Chem* **278**, 45154–9.
- Brown, G. C. (2001). Regulation of mitochondrial respiration by nitric oxide inhibition of cytochrome c oxidase. *Biochim Biophys Acta* **1504**, 46–57.
- Burcham, P. C. (1998). Genotoxic lipid peroxidation products: their DNA damaging properties and role in formation of endogenous DNA adducts. *Mutagenesis* **13**, 287–305.
- Burke, B. E., Mushlin, P. S., Cusack, B. J., Olson, S. J., Gambliel, H. A., and Olson, R. D. (2002). Decreased sensitivity of neonatal rabbit sarcoplasmic reticulum to anthracycline cardiotoxicity. *Cardiovasc Toxicol* **2**, 41–51.
- Burke, B. E., Olson, R. D., Cusack, B. J., Gambliel, H. A., and Dillmann, W. H. (2003). Anthracycline cardiotoxicity in transgenic mice overexpressing SR Ca<sup>2+</sup>-ATPase. *Biochem Biophys Res Commun* **303**, 504–7.
- Chiarpotto, E., Domenicotti, C., Paola, D., Vitali, A., Nitti, M., Pronzato, M. A., Biasi, F., Cottalasso, D., Marinari, U. M., Dragonetti, A., Cesaro, P., Isidoro, C., and Poli, G. (1999). Regulation of rat hepatocyte protein kinase C beta isoenzymes by the lipid peroxidation product 4-hydroxy-2,3-nonenal: a signaling pathway to modulate vesicular transport of glycoproteins. *Hepatology* **29**, 1565–72.
- Costa, N. J., Dahm, C. C., Hurrell, F., Taylor, E. R., and Murphy, M. P. (2003). Interactions of mitochondrial thiols with nitric oxide. *Antioxid Redox Signal* **5**, 291–305.
- Cotran, R. S., Kumar, V., and Collins, T. (1999). *Robbins Pathologic Basis of Disease*. 6th ed. W. B. Saunders, Philadelphia.
- Cummings, J., Anderson, L., Willmott, N., and Smyth, J. F. (1991). The molecular pharmacology of doxorubicin in vivo. *Eur J Cancer* **27**, 532–5.
- Curzio, M. (1988). Interaction between neutrophils and 4-hydroxyalkenals and consequences on neutrophil motility. *Free Radic Res Commun* **5**, 55–66.
- Dianzani, M. U. (1998). 4-Hydroxynonenal and cell signalling. *Free Radic Res* **28**, 553–60.
- Doorn, J. A., and Petersen, D. R. (2002). Covalent modification of amino acid nucleophiles by the lipid peroxidation products 4-hydroxy-2-nonenal and 4-oxo-2-nonenal. *Chem Res Toxicol* **15**, 1445–50.
- Doroshov, J. H. (1983). Effect of anthracycline antibiotics on oxygen radical formation in rat heart. *Cancer Res* **43**, 460–72.
- Doroshov, J. H., Tallent, C., and Schechter, J. E. (1985). Ultrastructural features of adriamycin-induced skeletal and cardiac muscle toxicity. *Am J Pathol* **118**, 288–97.
- Dziegiel, P., Surowiak, P., and Zabel, M. (2002). Correlation of histopathological and biochemical appraisal of anthracycline-induced myocardium damage. *Folia Histochem Cytobiol* **40**, 127–8.
- Fleurbaey-Morel, P., Barrier, L., Fauconneau, B., Piriou, A., and Huguet, F. (1999). Origin of 4-hydroxynonenal incubation-induced inhibition of dopamine transporter and Na<sup>+</sup>/K<sup>+</sup> adenosine triphosphate in rat striatal synaptosomes. *Neurosci Lett* **277**, 91–4.
- Forrest, G. L., Gonzalez, B., Tseng, W., Li, X., and Mann, J. (2000). Human carbonyl reductase overexpression in the heart advances the development of doxorubicin-induced cardiotoxicity in transgenic mice. *Cancer Res* **60**, 5158–64.
- Gosalvez, M., Blanco, M., Hunter, J., Miko, M., and Chance, B. (1974). Effects of anticancer agents on the respiration of isolated mitochondria and tumor cells. *Eur J Cancer* **10**, 567–74.
- Granger, D. L., and Lehninger, A. L. (1983). Sites of inhibition of mitochondrial electron transport in macrophage-injured neoplastic cells. *J Cell Biol* **95**, 527–35.
- Grune, T., Reinheckel, T., Joshi, M., and Davies, K. J. (1995). Proteolysis in cultured liver epithelial cells during oxidative stress. Role of the multicatalytic proteinase complex, proteasome. *J Biol Chem* **270**, 2344–51.
- Hahm, S., Dresner, H. S., Podwall, D., Golden, M., Winiarsky, R., Moosikasowan, M., Cajigas, A., and Steinberg, J. J. (2003). DNA biomarkers antecede semiquantitative anthracycline cardiomyopathy. *Cancer Invest* **21**, 53–67.
- Halliwell, B. (1997). What nitrates tyrosine? Is nitrotyrosine specific as a biomarker of peroxynitrite formation in vivo? *FEBS Lett* **411**, 157–60.
- Hanafy, K. A., Krumenacker, J. S., and Murad, F. (2001). NO, nitrotyrosine, and cyclic GMP in signal transduction. *Med Sci Monit* **7**, 801–19.
- Hrelia, S., Fiorentini, D., Maraldi, T., Angeloni, C., Bordoni, A., Biagi, P. L., and Hakim, G. (2002). Doxorubicin induces early lipid peroxidation associated with changes in glucose transport in cultured cardiomyocytes. *Biochim Biophys Acta* **1567**, 150–6.
- Ito, H., C., M. S., Billingham, M. E., Akimoto, H., Torti, S. V., Wade, R., Gahlmann, R., Lyons, G., Kedes, L., and Torti, F. M. (1990). Doxorubicin selectively inhibits muscle gene expression in cardiac muscle cells in vivo and in vitro. *Proc Natl Acad Sci USA* **87**, 4275–9.
- Kirsch, M., Korth, H. G., Sustmann, R., and Groot, H. (2002). The pathobiochemistry of nitrogen dioxide. *Biol Chem* **383**, 389–99.
- Kong, S. K., Yim, M. B., Stadtman, E. R., and Chock, P. B. (1996). Peroxynitrite disables the tyrosine phosphorylation regulatory mechanism: lymphocyte-specific tyrosine kinase fails to phosphorylate nitrated cdc2(6-20)/NH2 peptide. *Proc Natl Acad Sci USA* **93**, 3377–82.
- Kwok, J. C., and Richardson, D. R. (2002). Unexpected anthracycline-mediated alterations in iron-regulatory protein-RNA-binding activity: the iron and copper complexes of anthracyclines decrease RNA-binding activity. *Mol Pharmacol* **62**, 888–900.

- Lambertenghi-Deliliers, G., Zanon, P. L., Pozzoli, E. F., and Bellini, O. (1976). Myocardial injury induced by a single dose of adriamycin: an electron microscopic study. *Tumori* **62**, 517–28.
- Merski, J., Daskal, Y., and Busch, H. (1978). Comparison of adriamycin-induced nucleolar segregation in skeletal muscle, cardiac muscle, and liver cells. *Cancer Treat Rep* **62**, 771–8.
- Merski, J. A., Daskal, I., and Busch, H. (1976). Effects of adriamycin on ultrastructure of nucleoli in the heart and liver cells of the rat. *Cancer Res* **36**, 1580–4.
- Metzen, E., Zhou, J., Jelkmann, W., Fandrey, J., and Brune, B. (2003). Nitric oxide impairs normoxic degradation of HIF-1 $\alpha$  by inhibition of prolyl hydroxylases. *Mol Biol Cell* **14**, 3470–81.
- Mihm, M. J., Yu, F., Weinstein, D. M., Reiser, P. J., and Bauer, J. A. (2002). Intracellular distribution of peroxynitrite during doxorubicin cardiomyopathy: evidence for selective impairment of myofibrillar creatine kinase. *Br J Pharmacol* **135**, 581–8.
- Mikkelsen, R. B., and Wardman, P. (2003). Biological chemistry of reactive oxygen and nitrogen and radiation-induced signal transduction mechanisms. *Oncogene* **22**, 5734–54.
- Nguyen, E., and Picklo, M. J. S. (2003). Inhibition of succinic semialdehyde dehydrogenase activity by alkenal products of lipid peroxidation. *Biochim Biophys Acta* **1637**, 107–12.
- Oberley, T. D. (2002). Ultrastructural localization and relative quantification of 4-hydroxynonenal-modified proteins in tissues and cell compartments. *Meth Enzymol* **352**, 373–7.
- Page, S., Fischer, C., Baumgartner, B., Haas, M., Kreusel, U., Loidl, G., Hayn, M., Ziegler-Heitbrock, H. W., Neumeier, D., and Brand, K. (1999). 4-Hydroxynonenal prevents NF- $\kappa$ B activation and tumor necrosis factor expression by inhibiting I $\kappa$ B phosphorylation and subsequent proteolysis. *J Biol Chem* **274**, 11611–8.
- Paola, D., Domenicotti, C., Nitti, M., Vitali, A., Borghi, R., Cottalasso, D., Zaccheo, D., Odetti, P., Strocchi, P., Marinari, U. M., Tabaton, M., and Pronzato, M. A. (2000). Oxidative stress induces increase in intracellular amyloid beta-protein production and selective activation of beta I and beta II PKCs in NT2 cells. *Biochem Biophys Res Commun* **268**, 642–6.
- Parola, M., Pinzani, M., Casini, A., Albano, E., Poli, G., Gentilini, A., Gentilini, P., and Dianzani, M. U. (1993). Stimulation of lipid peroxidation or 4-hydroxynonenal treatment increases procollagen alpha 1 (I) gene expression in human liver fat-storing cells. *Biochem Biophys Res Commun* **194**, 1044–50.
- Paxinou, E., Weisse, M., Chen, Q., Souza, J. M., Hertkorn, C., Selak, M., Daikhin, E., Yudkoff, M., Sowa, G., Sessa, W. C., and Ischiropoulos, H. (2001). Dynamic regulation of metabolism and respiration by endogenously produced nitric oxide protects against oxidative stress. *Proc Natl Acad Sci USA* **98**, 11575–80.
- Poli, G., Dianzani, M. U., Cheeseman, K. H., Slater, T. F., Lang, J., and Esterbauer, H. (1985). Separation and characterization of the aldehydic products of lipid peroxidation stimulated by carbon tetrachloride or ADP-iron in isolated rat hepatocytes and rat liver microsomal suspensions. *Biochem J* **277**, 629–38.
- Reinheckel, T., Noack, H., Lorenz, S., Wiswedel, I., and Augustin, W. (1998). Comparison of protein oxidation and aldehyde formation during oxidative stress in isolated mitochondria. *Free Radic Res* **29**, 297–305.
- Revis, N. W., and Marusic, N. (1979). Effects of doxorubicin and its aglycone metabolite on calcium sequestration by rabbit heart, liver, and kidney mitochondria. *Life Sci* **25**, 1055–63.
- Sato, S., Iwaizumi, M., Handa, K., and Tamura, Y. (1977). Electron spin resonance study on the mode of generation of free radicals of daunomycin, adriamycin, and carboquone in NAD(P)H-microsome system. *Gann* **68**, 603–8.
- Singhal, S. S., Singhal, J., Sharma, R., Singh, S. V., Zimniak, P., Awasthi, Y. C., and Awasthi, S. (2003). Role of RLIP76 in lung cancer doxorubicin resistance: I. The ATPase activity of RLIP76 correlates with doxorubicin and 4-hydroxynonenal resistance in lung cancer cells. *Int J Oncol* **22**, 365–75.
- Spitz, D. R., Sullivan, S. J., Malcolm, R. R., and Roberts, R. J. (1991). Glutathione dependent metabolism and detoxification of 4-hydroxy-2-nonenal. *Free Radic Biol Med* **11**, 415–23.
- Thomas, D. D., Miranda, K. M., Colton, C. A., Citrin, D., Espey, M. G., and Wink, D. A. (2003). Heme proteins and nitric oxide (NO): the neglected, eloquent chemistry in NO redox signaling and regulation. *Antioxid Redox Signal* **5**, 307–17.
- Toyokuni, S., Uchida, K., Okamoto, K., Hattori-Nakakuki, Y., Hiai, H., and Stadtman, E. R. (1994). Formation of 4-hydroxy-2-nonenal-modified proteins in the renal proximal tubules of rats treated with a renal carcinogen, ferric nitrilotriacetate. *Proc Natl Acad Sci USA* **91**, 2616–20.
- Tsai, L., Szweda, P. A., Vinogradova, O., and Szweda, L. I. (1998). Structural characterization and immunochemical detection of a fluorophore derived from 4-hydroxy-2-nonenal and lysine. *Proc Natl Acad Sci USA* **95**, 7975–80.
- Uchida, K., Szweda, L. I., Chae, H.-Z., and Stadtman, E. R. (1993). Immunochemical detection of 4-hydroxy-2-nonenal protein adducts in oxidized hepatocytes. *Proc Natl Acad Sci USA* **90**, 8742–6.
- Weinstein, D. M., Mihm, M. J., and Bauer, J. A. (2000). Cardiac peroxynitrite formation and left ventricular dysfunction following doxorubicin treatment in mice. *J Pharmacol Exp Ther* **294**, 396–401.
- Willard, B. B., Ruse, C. I., Keightley, J. A., Bond, M., and Kinter, M. (2003). Site-specific quantitation of protein nitration using liquid chromatography/tandem mass spectrometry. *Anal Chem* **75**, 2370–6.
- Yen, H. C., Oberley, T. D., Gairola, C. G., Szweda, L. I., and St. Clair, D. K. (1999). Manganese superoxide dismutase protects mitochondrial complex I against adriamycin-induced cardiomyopathy in transgenic mice. *Arch Biochem Biophys* **362**, 59–66.
- Yen, H. C., Oberley, T. D., Vichitbandha, S., Ho, Y. S., and St. Clair, D. K. (1996). The protective role of manganese superoxide dismutase against adriamycin-induced acute cardiac toxicity in transgenic mice. *J Clin Invest* **98**, 1253–60.
- Zainal, T. A., Oberley, T. D., Allison, D. B., Szweda, L. I., and Weindruch, R. (2000). Caloric restriction of Rhesus monkeys lowers oxidative damage in skeletal muscle. *FASEB J* **14**, 1825–39.
- Zainal, T. A., Weindruch, R., Szweda, L. I., and Oberley, T. D. (1999). Localization of 4-hydroxy-2-nonenal-modified proteins in kidney following iron overload. *Free Radic Biol Med* **26**, 1181–93.